3. Mathematical Analysis of Air Gap Fields

3.1 Fundamental and Harmonics of Air Gap Fields

Waves and oscillations are basically different: The amplitude of (periodic) **wave** changes periodically with **space and time**, whereas in case of an **oscillation** it changes **only with time**. Therefore, the field distribution in the air gap $B_\delta(x,t)$ is a wave, whereas the alternating current per phase $i(t)$ is an oscillation.

The "step-like" shape of the graph of the travelling wave $B_\delta(x,t)$ in the air gap (Fig. 2.8) changes its form periodically (with the period time $T/6$) as it travels. Only the **fundamental wave** of the travelling field is of interest. This wave has the wavelength $2\tau_p$ and does NOT change its shape as it travels. Therefore, it can be easily used for electromechanical energy conversion. The fundamental wave can be determined from $B_\delta(x,t)$ by means of the ***FOURIER*-analysis.** Furthermore, $B_\delta(x,t)$ contains **harmonic waves** with shorter wavelengths and smaller amplitudes than the fundamental. These are considered as parasitic effects that – generally – only interfere with the main purpose of the electric machine, which is the electromechanical energy conversion. The harmonics are also the reason for the change of the field distribution as it travels onwards.

a) Rotating Waves, Travelling Waves:
The **fundamental wave** has the following mathematical expression

$$\boxed{B_{\delta 1}(x,t) = \hat{B}_{\delta 1}\cos\left(\frac{x\cdot\pi}{\tau_p} - 2\pi f\cdot t\right)} \qquad (3.1)$$

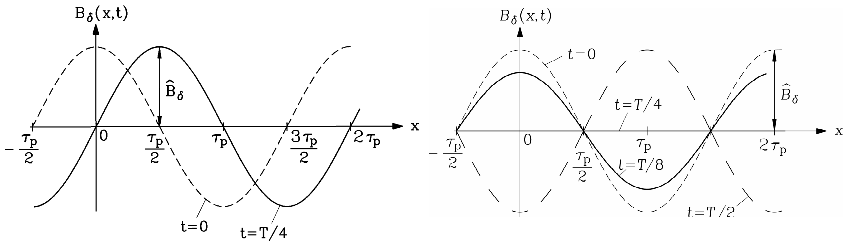

a) b)

Fig. 3.1: Waves of the magnetic field in the air gap: a) fundamental wave of the field distribution of Fig. 2.8 as travelling wave, b) standing wave as fundamental of the field distribution of the phase of a winding of Fig. 2.7

At the time $t = 0$, the fundamental is a cosine function with the maximum value obtained at $x = 0$ (Fig 3.1a).

$$B_{\delta 1}(x,0) = \hat{B}_{\delta 1}\cos\left(\frac{x\cdot\pi}{\tau_p}\right)$$

At the time $t = T/4$ (where $T = 1/f$), it is a sine function with the maximum value given at $x = \tau_p/2$.

$$B_{\delta 1}(x,T/4) = \hat{B}_{\delta 1}\cos\left(\frac{x\cdot\pi}{\tau_p} - \frac{\pi}{2}\right) = \hat{B}_{\delta 1}\sin\left(\frac{x\cdot\pi}{\tau_p}\right)$$

The wave has travelled the distance of $\tau_p/2$. At a fixed coordinate $x = C$, the flux density oscillates with the frequency f, but with a different phase $C\pi/\tau_p$.

$$B_{\delta 1}(x = C,t) = \hat{B}_{\delta 1}\cos\left(\frac{C\cdot\pi}{\tau_p} - 2\pi f\cdot t\right)$$

The circumferential speed v_{syn} of the rotating wave (or, in case of a linear motor, the velocity v of the travelling wave) is calculated in a way that an observer who travels with the wave always sees a constant phase $\frac{x\pi}{\tau_p} - 2\pi f t = cst.$. Therefore, for the observer it is

$$v_{syn} = \frac{dx}{dt} = \frac{d}{dt}(cst. + 2\pi f t)\frac{\tau_p}{\pi} = 2f\tau_p$$

This result was already derived in Chapter 2 in a different way. Accordingly, a wave travelling in **opposite direction** $v_{syn} = -2f\tau_p$ has the following mathematical expression

$$B_{\delta 1}(x,t) = \hat{B}_{\delta 1}\cos\left(\frac{x\cdot\pi}{\tau_p} + 2\pi f\cdot t\right) \qquad \text{"reverse rotating field"} \qquad (3.1a)$$

Example 3.1-1:
At $f = 50$ Hz, v_{syn} in m/s has the same numerical value as the pole pitch in cm.

$f = 50$ Hz : $\quad v_{syn}^{[m/s]} = \tau_p^{[cm]}$

Two-pole turbo generator ($2p = 2$) used in a thermal power plant: $n_{syn} = 3000$/min:
- bore diameter $d_{si} = 1.2$ m
- pole pitch $\tau_p = 1.2\pi/2 = 1.88$ m = 188 cm
- v_{syn} = 188 m/s = 676 km/h = circumferential speed of the rotor which rotates synchronously with the rotating field (synchronous machine!)

b) Standing Waves:
The field distribution of a phase supplied with alternating current (e.g. Fig. 2.7) does not travel, but "stands" spatially fixed, pulsating with the frequency f during time. The *FOURIER*-fundamental is also a standing, pulsating wave (Fig. 3.1b).

$$\boxed{B_{\delta 1}(x,t) = \hat{B}_{\delta 1}\cos\left(\frac{x\cdot\pi}{\tau_p}\right)\cdot\cos(2\pi f\cdot t)} \qquad (3.2)$$

This wave does not change the location of its nodes (zeros) and antinodes (maxima), however, the amplitude pulsates. At the time $t = 0$, the maximum at $x = 0$ has the value $\hat{B}_{\delta 1}$, at $t = T/8$ only $\hat{B}_{\delta 1}/\sqrt{2}$, at $t = T/4$ zero, at $t = T/2$ $-\hat{B}_{\delta 1}$ etc.

3.2 *FOURIER*-Analysis for Determination of Fundamental and Harmonics

A periodic function $V(\gamma)$ with period 2π can be described as an infinite sum of sinusoidal functions (*FOURIER*-series):

$$V(\gamma) = V_0 + \sum_{\nu=1,2,3,...}^{\infty} \left[\hat{V}_{\nu,a} \cdot \cos(\nu \cdot \gamma) + \hat{V}_{\nu,b} \cdot \sin(\nu \cdot \gamma) \right] \tag{3.3}$$

The individual amplitudes of the ordinal numbers

$$\nu = 1, 2, 3, ... \tag{3.4}$$

are calculated using

$$\hat{V}_{\nu,a} = \frac{1}{\pi} \int_0^{2\pi} V(\gamma) \cdot \cos(\nu \cdot \gamma) \cdot d\gamma, \quad \hat{V}_{\nu,b} = \frac{1}{\pi} \int_0^{2\pi} V(\gamma) \cdot \sin(\nu \cdot \gamma) \cdot d\gamma, \tag{3.5}$$

and the average value is calculated using

$$V_0 = \frac{1}{2\pi} \int_0^{2\pi} V(\gamma) \cdot d\gamma . \tag{3.6}$$

a) FOURIER-Analysis of the Field of a Fully-Pitched Coil (q = 1):
According to Fig. 3.2a, the spatial distribution of the magnetic voltage $V_c(x)$ of a winding branch with $q = 1$ coils per pole and phase is – independently of the time dependence of the coil current i_c – a rectangular function. In case of a two-layer winding, each slot provides the "concentrated" slot ampere-turns $\Theta_Q = 2N_c i_c$. The circumferential coordinate x is expressed by the circumferential angle γ

$$\boxed{\gamma = x\frac{\pi}{\tau_p}}. \tag{3.7}$$

At $x = 2\tau_p$, the circumferential angle is 2π. In the case of a two-pole machine, this equals the circumferential angle 2π in **"mechanical degrees"**. However, in the case of a four-pole machine, it corresponds only to a circumferential angle of π in "mechanical degrees" etc. Hence, the circumferential angle γ is counted in **"electric degrees"**. Generally, 2π "electric degrees" equal $2\pi/p$ "mechanical degrees".

As the negative and the positive areas of the graph $V_c(\gamma)$ have the same magnitude, $V_{c,0}$ is zero according to (3.6): **The air gap field does not contain a constant component, so no unipolar flux density occurs.** If the position of $\gamma = 0$ is chosen as shown in Fig. 3.2a, $V_c(\gamma)$ is an **"even" function**, and it is:

$$V_c(\gamma) = V_c(-\gamma) \tag{3.8}$$

Combining (3.8) and (3.5) shows that $\hat{V}_{c,\nu,b} = 0$ (Please verify by yourself!).

Result:
If the FOURIER-analysis of an even function is done, the FOURIER-sum contains only cosine-functions.

Furthermore, the field graph of Fig. 3.2 is symmetrical to the abscissa:

$$V_c(\gamma) = -V_c(\gamma + \pi) \quad . \tag{3.9}$$

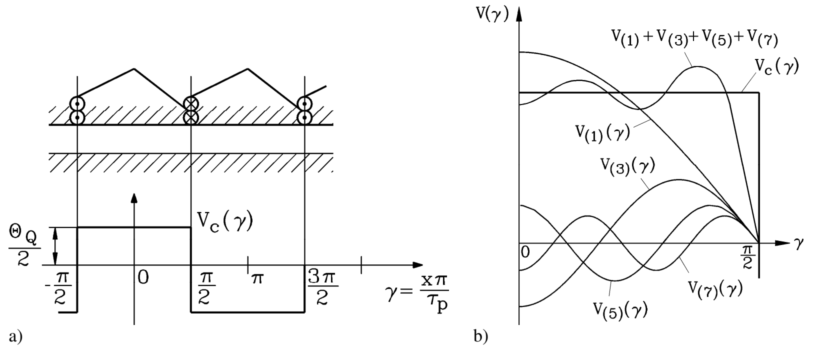

Fig. 3.2: a) magnetic voltage $V_c(x)$ of a series of fully-pitched, current-carrying coils, b) fundamental $\nu = 1$ and harmonics $\nu = 3, 5, 7$ as well as their sum

Combining (3.9) and (3.5) gives for $\nu = 1, 2, 3, ...$:

$$V_{c,\nu,a} = \frac{1}{\pi} \int_0^{2\pi} V_c(\gamma) \cos(\nu\gamma) d\gamma = \frac{1}{\pi} \int_0^{\pi} V_c(\gamma) \cos(\nu\gamma) d\gamma + \frac{1}{\pi} \int_{\pi}^{2\pi} V_c(\gamma) \cos(\nu\gamma) d\gamma \tag{3.10}$$

Using the symmetry to the abscissa, the second integral gives:

$$\int_{\pi}^{2\pi} V_c(\gamma) \cos(\nu\gamma) d\gamma = \int_0^{\pi} V_c(\gamma' + \pi) \cos(\nu(\gamma' + \pi)) d\gamma' = \int_0^{\pi} -V_c(\gamma') \cos(\nu\gamma') (-1)^{\nu} d\gamma' \tag{3.11}$$

Thus, in the case of even ordinal numbers, the first and the second integral cancel each other:

$$\nu = 2, 4, 6, ...: \quad \hat{V}_{c,\nu,a} = \frac{1}{\pi} \left[\int_0^{\pi} V_c(\gamma) \cos(\nu\gamma) d\gamma - \int_0^{\pi} V_c(\gamma) \cos(\nu\gamma) d\gamma \right] = 0 \tag{3.12}$$

It remains:

$$\nu = 1, 3, 5, ...: \quad \hat{V}_{c,\nu,a} = \frac{1}{\pi} \left[\int_0^{\pi} V_c(\gamma) \cos(\nu\gamma) d\gamma + \int_0^{\pi} V_c(\gamma) \cos(\nu\gamma) d\gamma \right] = \frac{2}{\pi} \int_0^{\pi} V_c(\gamma) \cos(\nu\gamma) d\gamma \tag{3.13}$$

Result:
Graphs such as field distributions symmetrical to the abscissa only have harmonics with odd ordinal numbers.

$$\boxed{\hat{V}_{c,\nu} = \frac{2}{\pi} \int_0^{\pi} V_c(\gamma) cos(\nu\gamma) d\gamma, \qquad V_c(\gamma) = \sum_{\nu=1,3,5,...}^{\infty} \hat{V}_{c,\nu} \, cos(\nu\gamma)} \tag{3.14}$$

Ultimately, the *FOURIER*-analysis of the rectangular function results in (Please verify by yourself!):

$$\boxed{\hat{V}_{c,\nu} = \frac{2}{\pi} \int_0^{\pi} V_c(\gamma) \cos(\nu\gamma) d\gamma = \frac{\Theta_Q}{2} \cdot \frac{4}{\nu\pi} \cdot \sin\left(\frac{\nu\pi}{2}\right)}, \quad \nu = 1, 3, 5, ... \quad . \tag{3.15}$$

As the factor $\sin(\nu\pi/2)$ always has the absolute value 1, the amplitudes of the harmonics decrease with $1/\nu$. The finite *FOURIER*-sum up to the 7$^{\text{th}}$ harmonic describes the rectangular distribution relatively well (Fig. 3.2b).

b) FOURIER-Analysis of the Field of Short-Pitched Coils (q = 1):

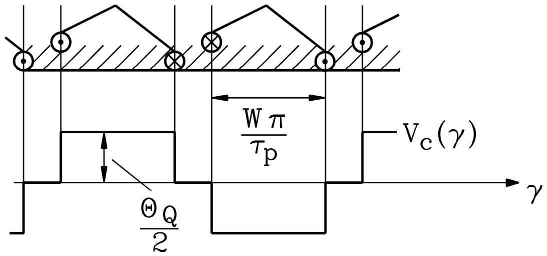

Fig. 3.3: Magnetic voltage $V_c(x)$ of a series of short-pitched, current-carrying coils

If the coils are short-pitched, $V_c(x)$ changes as shown in Fig. 3.3. The corresponding calculation of the *FOURIER*-amplitudes is (Please verify by yourself!):

$$\hat{V}_{c,\nu} = \frac{2}{\pi}\int_0^{\pi} V_c(\gamma)\cos(\nu\gamma)d\gamma = \frac{\Theta_Q}{2}\cdot\frac{4}{\nu\pi}\cdot\sin\left(\frac{W}{\tau_p}\cdot\frac{\nu\pi}{2}\right), \qquad \nu = 1, 3, 5, \ldots \qquad (3.16)$$

When compared with fully-pitched coils, the absolute value of the amplitudes is reduced by the **"pitch factor"** $k_{p,\nu}$.

$$\boxed{k_{p,\nu} = \sin\left(\frac{W}{\tau_p}\cdot\frac{\nu\pi}{2}\right)} \qquad (3.17)$$

In the particular case $W = \tau_p$ ("fully-pitched"), (3.16) becomes (3.15).

c) FOURIER-Analysis of the Field of Fully-Pitched Coil Groups (q > 1):
Fig. 3.4 shows the distribution of the magnetic voltage of a fully-pitched coil group for $q = 2$. The *FOURIER*-analysis of the distribution of the magnetic voltage $V_{gr}(\gamma)$ is

$$\hat{V}_{gr,\nu} = \frac{2}{\pi}\int_0^{\pi} V_{gr}(\gamma)\cos(\nu\gamma)d\gamma = \frac{q\Theta_Q}{2}\cdot\frac{4}{\nu\pi}\cdot\sin\left(\frac{\nu\pi}{2}\right)\cdot\frac{\sin(\frac{\nu\pi}{2m})}{q\cdot\sin(\frac{\nu\pi}{2mq})}, \qquad \nu = 1, 3, 5, \ldots \qquad (3.18)$$

where stance between two adjacent slots of $\tau_Q = \tau_p/(mq)$ was considered. When comparing (3.18) with (3.15), the amplitudes are

- larger by the factor q, because the number of ampere-turns per slot increases by a factor q,
- but on the other hand they are reduced by the **"distribution factor"** $k_{d,\nu}$.

$$\boxed{k_{d,\nu} = \frac{\sin(\frac{\nu\pi}{2m})}{q\cdot\sin(\frac{\nu\pi}{2mq})}} \qquad (3.19)$$

In the particular case $q = 1$ (3.18) becomes (3. 15).

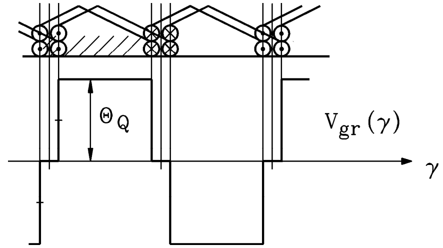

Fig. 3.4: Magnetic voltage $V_{gr}(x)$ of a series of fully-pitched, current-carrying coil groups (example: $q = 2$; therefore amplitude $q\Theta_Q/2 = \Theta_Q$)

With the number of windings per phase N and the current per coil i_c expressed by the current per phase $i = a.i_c$, the ampere-turns can be expressed as follows:

$$\frac{q\Theta_Q}{2} = qN_c i_c = \frac{2pqN_c}{a}\cdot\frac{ai_c}{2p} = N\cdot\frac{i}{2p} \qquad (3.20)$$

Of course, the current per coil and the current per phase are the same in the particular case of a series connection of all coils ($a = 1$). Using (3.20), the amplitudes of (3.18) become:

$$\hat{V}_{gr,\nu} = N\cdot\frac{i}{2p}\cdot\frac{4}{\nu\pi}\cdot\sin\left(\frac{\nu\pi}{2}\right)\cdot k_{d,\nu} \qquad (3.21)$$

d) FOURIER-Analysis of the Field of a Short-Pitched Winding Branch (q > 1, W/τ$_p$ < 1):
In the general case of a series of short-pitched coil groups, the expression $\sin(\nu\pi/2)$ in (3.21) has to be replaced by the pitch factor. Thereby, the *FOURIER*-analysis of the graph $V_{ph}(\gamma)$ of a winding branch is obtained:

$$\hat{V}_{ph,\nu} = N\cdot\frac{i}{2p}\cdot\frac{4}{\nu\pi}\cdot k_{p,\nu}\cdot k_{d,\nu}, \quad \nu = 1, 3, 5, \ldots \qquad (3.22)$$

Result:
The FOURIER-analysis of the magnetic voltage distribution $V_{ph}(\gamma,t)$, hence the distribution of the magnetic flux density $B_\delta(x,t)$ of an individual winding branch with the number of turns N, carrying the current $i = I\cdot\sqrt{2}\cdot\cos(\omega t)$, results in equations (3.23) and (3.24). The distribution of the magnetic voltage is given by the sum of standing, pulsating harmonic waves as "alternating fields".

$$\boxed{\hat{V}_{ph,\nu} = \frac{2\cdot\sqrt{2}}{\pi}\cdot\frac{N}{p}\cdot\frac{1}{\nu}\cdot k_{p,\nu}\cdot k_{d,\nu}\cdot I}, \qquad \nu = 1, 3, 5, \ldots \qquad (3.23)$$

$$\boxed{V_{ph}(\gamma,t) = \sum_{\nu=1,3,5,\ldots}^{\infty}\hat{V}_{ph,\nu}\cdot\cos(\nu\gamma)\cdot\cos(\omega t)} \qquad (3.24)$$

The product of pitch and distribution factor is called **"winding factor"** $k_{w,\nu}$.

$$k_{w,\nu} = k_{p,\nu} \cdot k_{d,\nu} \quad (3.25)$$

Example 3.2-1:
Pitch, distribution and winding factors of three frequently used three-phase windings A, B, C for selected ordinal numbers:

	A			B			C		
	$q = 1$, $W/\tau_p = 2/3$			$q = 2$, $W/\tau_p = 5/6$			$q = 3$, $W/\tau_p = 7/9$		
	$Q/p = 6$			$Q/p = 12$			$Q/p = 18$		
ν	$k_{p,\nu}$	$k_{d,\nu}$	$k_{w,\nu}$	$k_{p,\nu}$	$k_{d,\nu}$	$k_{w,\nu}$	$k_{p,\nu}$	$k_{d,\nu}$	$k_{w,\nu}$
1	0.866	1	0.866	0.966	0.966	0.933	0.940	0.960	0.902
5	-0.866	1	-0.866	0.259	0.259	0.067	-0.174	0.218	-0.038
7	0.866	1	0.866	0.259	-0.259	-0.067	0.766	-0.177	-0.136
11	-0.866	1	-0.866	0.966	-0.966	-0.933	0.766	-0.177	-0.136
13	0.866	1	0.866	-0.966	-0.966	0.933	-0.174	0.218	-0.038
17	-0.866	1	-0.866	-0.259	-0.259	0.067	0.940	0.960	0.902
19	0.866	1	0.866	-0.259	0.259	-0.067	-0.940	0.960	-0.902

Table 3.1: Pitch, distribution and winding factors of short-pitched three-phase windings with 6, 12 and 18 slots per pole pair

The table shows that, because of the sine function, the winding factors periodically have the same magnitude also at bigger ν (even at $q > 1$) as at ordinal number $\nu = 1$.

e) FOURIER-Analysis of the Field of a Three-Phase Winding:
The **standing, pulsating distribution of the magnetic voltage** per phase is expressed for all three, spatially by $2\tau_p/3$ distributed phases, U, V, W individually for each ordinal number ν. Thereby, all phases are supplied with three sinusoidal alternating currents with $T/3$ phase displacement.

$$V_{U\nu}(\gamma,t) = \hat{V}_{ph,\nu} \cdot \cos(\nu\gamma) \cdot \cos(\omega t) \quad (3.26)$$

$$V_{V\nu}(\gamma,t) = \hat{V}_{ph,\nu} \cdot \cos(\nu(\gamma - 2\pi/3)) \cdot \cos(\omega t - 2\pi/3) \quad (3.27)$$

$$V_{W\nu}(\gamma,t) = \hat{V}_{ph,\nu} \cdot \cos(\nu(\gamma - 4\pi/3)) \cdot \cos(\omega t - 4\pi/3) \quad (3.28)$$

The standing, pulsating waves (3.26) – (3.28) can be decomposed into **a positive and a negative - sequence** rotating field, using the trigonometric law

$$\cos\alpha \cdot \cos\beta = \frac{1}{2} \cdot [\cos(\alpha+\beta) + \cos(\alpha-\beta)] \;.$$

$$V_{U\nu}(\gamma,t) = \frac{\hat{V}_{ph,\nu}}{2}\cos(\nu\gamma + \omega t) + \frac{\hat{V}_{ph,\nu}}{2}\cos(\nu\gamma - \omega t) \quad (3.29)$$

$$V_{V\nu}(\gamma,t) = \frac{\hat{V}_{ph,\nu}}{2}\cos(\nu\gamma - \frac{\nu 2\pi}{3} + \omega t - \frac{2\pi}{3}) + \frac{\hat{V}_{ph,\nu}}{2}\cos(\nu\gamma - \frac{\nu 2\pi}{3} - \omega t + \frac{2\pi}{3}) \quad (3.30)$$

$$V_{W\nu}(\gamma,t) = \frac{\hat{V}_{ph,\nu}}{2}\cos(\nu\gamma - \frac{\nu 4\pi}{3} + \omega t - \frac{4\pi}{3}) + \frac{\hat{V}_{ph,\nu}}{2}\cos(\nu\gamma - \frac{\nu 4\pi}{3} - \omega t + \frac{4\pi}{3}) \quad (3.31)$$

In the following, the sum

$$V(\gamma,t) = \sum_{\nu=1,3,5,\dots}^{\infty} (V_{U\nu}(\gamma,t) + V_{V\nu}(\gamma,t) + V_{W\nu}(\gamma,t)) = \sum_{\nu=1,3,5,\dots}^{\infty} V_\nu(\gamma,t) \quad (3.32)$$

is expressed in detail for $\nu = 1$:

$$V_{U1}(\gamma,t) = \frac{\hat{V}_{ph,1}}{2}\cos(\gamma + \omega t) + \frac{\hat{V}_{ph,1}}{2}\cos(\gamma - \omega t)$$

$$V_{V1}(\gamma,t) = \frac{\hat{V}_{ph,1}}{2}\cos(\gamma + \omega t - \frac{4\pi}{3}) + \frac{\hat{V}_{ph,1}}{2}\cos(\gamma - \omega t)$$

$$V_{W1}(\gamma,t) = \frac{\hat{V}_{ph,1}}{2}\cos(\gamma + \omega t - \frac{8\pi}{3}) + \frac{\hat{V}_{ph,1}}{2}\cos(\gamma - \omega t)$$

Using the correlation

$$\cos(\lambda) + \cos(\lambda - \frac{4\pi}{3}) + \cos(\lambda - \frac{8\pi}{3}) = 0\,, \quad (3.33)$$

the first three addends (namely the negative - sequence waves) of the sum $V_1(\gamma,t) = V_{U1}(\gamma,t) + V_{V1}(\gamma,t) + V_{W1}(\gamma,t)$ cancel each other, whereas the second three addends (the positive - sequence waves !) add to each other to become the resultant rotating field that has **1.5-times the amplitude** when compared with the standing oscillating fields per phase:

$$V_1(x,t) = \frac{3}{2}\hat{V}_{ph,1}\cos(\gamma - \omega t) \quad (3.34)$$

Using $B_\delta = \mu_0 V/\delta$, the **fundamental of the rotating field** (as given in (3.1)) is obtained

$$B_{\delta 1}(x,t) = \hat{B}_{\delta 1}\cos\left(\frac{x \cdot \pi}{\tau_p} - 2\pi f \cdot t\right) \quad .$$

In the same way, the sum for $\nu > 1$ is calculated, resulting in

$$V_3(\gamma,t) = 0 + 0 = 0 \quad (3.35)$$

$$V_5(\gamma,t) = \frac{3}{2}\hat{V}_{ph,5}\cos(5\gamma + \omega t) \quad (3.36)$$

$$V_7(\gamma,t) = \frac{3}{2}\hat{V}_{ph,7}\cos(7\gamma - \omega t) \quad (3.37)$$

$$V_9(\gamma,t) = 0 + 0 = 0 \quad (3.38)$$

Note:
The sum of the three phases is always **zero** for ordinal numbers ν that are multiples of three. The three positive-sequence and negative-sequence rotating waves cancel each other.

$\underline{\nu = 3, 9, 15, 21, \dots:}$ $\quad V_\nu(\gamma,t) = V_{U\nu}(\gamma,t) + V_{V\nu}(\gamma,t) + V_{W\nu}(\gamma,t) = 0 \quad (3.39)$

For $\underline{\nu = 7, 13, 19, \dots}$, the three negative-sequence rotating waves cancel each other, as in the case of the fundamental, whereas the three positive-sequence rotating waves add to each other, thereby generating the field of the POSITIVE - sequence harmonics that travel in the direction of the fundamental field.

For $\underline{\nu = 5, 11, 17, \dots}$, the three positive-sequence rotating waves cancel each other, whereas the three negative-sequence rotating waves add to each other, thereby generating the NEGATIVE -sequence field.

Result:
A three-phase winding for rotating fields that is supplied by a symmetrical three-phase system generates a step-like distribution of the m.m.f. V(x,t), which is decomposed into a fundamental and harmonic waves. ***Only odd ordinal numbers*** *ν = 1, 5, 7, 11, 13, 17, 19, ... occur.*

$$\boxed{V(x,t)=\sum_{\nu}V_{\nu}(x,t)=\sum_{\nu}\frac{\sqrt{2}}{\pi}\frac{m}{p}N\frac{k_{w,\nu}}{\nu}I\cdot\cos\left(\frac{\nu\pi x}{\tau_p}-\omega t\right)} \tag{3.40}$$

$$\nu = 1, -5, 7, -11, 13, -17,... \tag{3.41}$$

The **ordinal numbers** used in (3.40) are **signed** (3.41) to label the direction of rotation – positive or negative – of the waves. The sign of the ordinal number does not influence the expression $k_{w,\nu}/\nu$, because the signs of numerator and denominator cancel each other. The general number of phases m is used in (3.40) (here: m = 3), because the calculations are also true for every m-phase winding which is supplied by an m-phase current system.

The ordinal numbers can be determined using (3.42):

$$\boxed{\nu = 1+2mg \qquad g = 0, \pm1, \pm2, \pm3, ...}, \qquad (g\text{: integer number}) \tag{3.42}$$

Example 3.2-2:
Ordinal numbers at m = 3: $\nu = 1+2\cdot3\cdot g = 1+6g$

g	0	-1	1	-2	2	...
ν	1	-5	7	-11	13	...

The speed of rotation of the harmonics decreases with $1/\nu$:

$$v_{syn,\nu} = 2f\frac{\tau_p}{\nu} \tag{3.43}$$

The amplitudes decrease with $k_{w,\nu}/\nu$, which is a stronger reduction than $1/\nu$, because it is $|k_{w,\nu}|<1$. The frequency of the harmonics is consistently the stator frequency f. It is the same for all harmonics.

Example 3.2-3:
Amplitude spectrum $\hat{B}_{\delta\nu}/\hat{B}_{\delta1} = \hat{V}_{\nu}/\hat{V}_1$ for three different windings A, B, C:

	A	*B*	*C*
	q = 1, W/τ_p = 2/3	q = 2, W/τ_p = 5/6	q = 3, W/τ_p = 7/9
	Q/p = 6	Q/p = 12	Q/p = 18
ν	$\hat{B}_{\delta\nu}/\hat{B}_{\delta1}$ (%)	$\hat{B}_{\delta\nu}/\hat{B}_{\delta1}$ (%)	$\hat{B}_{\delta\nu}/\hat{B}_{\delta1}$ (%)
1	100	100	100
-5	-20	1.4	-0.8
7	14.3	-1.0	-2.2
-11	-9.1	-9.1	-1.4
13	7.7	7.7	-0.3
-17	-5.6	-0.4	5.9
19	5.3	0.38	-5.3

Table 3.2: Relative field amplitudes inside the air gap for short-pitched three-phase windings with 6, 12 and 18 slots per pole pair

Winding A:
2/3-pitch, number of slots per pole and phase q = 1: The amplitudes of the harmonics are large and decrease only with $1/\nu$. At q = 1 pitching affects fundamental and harmonic likewise.

Winding B:
5/6-pitch, number of slots per pole and phase q = 2: The 5th and 7th harmonics are strongly reduced, as well as the 17th, 19th due to periodicity of the winding factor.

Winding C:
7/9-pitch, number of slots per pole and phase q = 3: Due to the finer slotting when compared with q = 2, the 11th and the 13th harmonics are also strongly reduced.

Result:
Short-pitching and finer slotting lead to a significant reduction of the harmonics and result in a step-like field distribution that approaches the ideal sinusoidal shape.

f) Harmonic Waves Due to Slotting ("slot harmonics"):
It is obvious in Tab. 3.2 that the amplitudes of the harmonics with ordinal numbers

$$\nu_Q = 1+\frac{Q}{p}g, \qquad g = \pm1, \pm2, \pm3,... \tag{3.44}$$

are increased. This is due to the fact that the winding factor of these harmonics is the same as of the fundamental (see Example 3.2-1).

Example 3.2-4:
Ordinal numbers of harmonics due to slotting:
a) Q/p = 12 : $\nu_Q = 1+12g = -11$, 13, -23, 25 etc.,
b) Q/p = 18: $\nu_Q = 1+18g = -17$, 19, -35, 37 etc. (compare with Tab. 3.2).

The longest wavelength of these **slot harmonics** is about the slot pitch: These harmonics are generated by the discrete distribution of ampere-turns in the slots. Graphically, this corresponds to the steps of the graph $V(x)$. In some cases, these harmonics can cause unpleasant magnetic sounds (**"siren sounds"**) due to vibration of the stator iron stack and remarkable losses due to eddy currents in massive conducting parts of the electric machine. They are to be reduced by further means (see lecture: "Motor Development for Electric Drive Systems").

3.3 *FOURIER*-Analysis of the Field of a Squirrel-Cage Winding

Squirrel-cage induction motors have a squirrel-cage winding in the rotor instead of a coil-winding. This cage-winding consists of Q_r *conductive* bars (copper, aluminium) which are arranged in Q_r equally spaced slots that are shorted by a *conductive* ring at each front side (Fig. 3.5a). At motor operation, a system of voltages with frequency f_r is induced in this squirrel-cage, thereby generating a symmetrical system of rotating currents – a sinusoidal current in each bar where each current has a phase shift towards the current of the neighbouring bar. Therefore, each bar is an **individual phase**, resulting in the number of phases Q_r. Hence, the phase-current is the **current in the bar**. Each bar is **half of a winding**. Therefore, the number of turns per winding per phase is N_r = ½ and the pitch and distribution factor of this type of winding are 1. With μ being the ordinal number of the harmonics of the field distribution of the squirrel-cage winding, the *FOURIER*-analysis of the step-like field becomes with

$$N \to 1/2, \quad m \to Q_r, \quad k_{w,\nu} \to 1, \quad I \to I_{bar}, \quad \nu \to \mu \tag{3.45}$$

in analogy to (3.40):

$$\boxed{V(x,t) = \sum_{\mu=1,\ldots}^{\infty} \frac{\sqrt{2}}{\pi}\frac{Q_r}{p}\frac{1}{2}\frac{1}{\mu} I_{bar} \cdot \cos\left(\frac{\mu \pi x}{\tau_p} - 2\pi f_r t\right)} \tag{3.46}$$

with the ordinal numbers

$$\boxed{\mu = 1 + \frac{Q_r}{p} g_r \qquad g_r = 0, \pm 1, \pm 2, \ldots} \tag{3.47}$$

<u>*Example 3.3-1:*</u>
Squirrel-cage winding with $Q_r = 28$ bars, $2p = 4$ (Fig. 3.5b):

- The system of bar currents is periodic (period: $Q_r/p = 14$ bars). Hence, 14 different currents exist in the bars. Each two currents have of opposite sign respectively, e.g. 1 and 8, 2 and 9 etc.
- The phase displacement of the bar currents of two neighbouring bars equals the **slot angle** $\alpha_Q = 2\pi p/Q_r = \pi/7$.

Explanatory statement: A four-pole field wave of the stator induces in bars 1 and 8 currents of opposite sign (phase displacement π). Accordingly, the phase shift of the bar currents in bars 2 to 7 has to be 1/7 of π.

Fig. 3.6 shows the corresponding distribution of the m.m.f. for the time $t = 0$. At this time, the bar current in bar 1 has its maximum value. The bar current in bar 2 is smaller about the factor $\cos\alpha_Q = 0.9$, the current in bar 3 about the factor $\cos(2\alpha_Q) = 0.62$ etc.. The approximation of the field distribution towards the aspired ideal sinusoidal shape because of the high number of phases is clearly to see. According to (3.44) and (3.47), all harmonics are harmonics due to the slotting, because the winding factors of the fundamental and of the harmonics are the same, which is always 1.

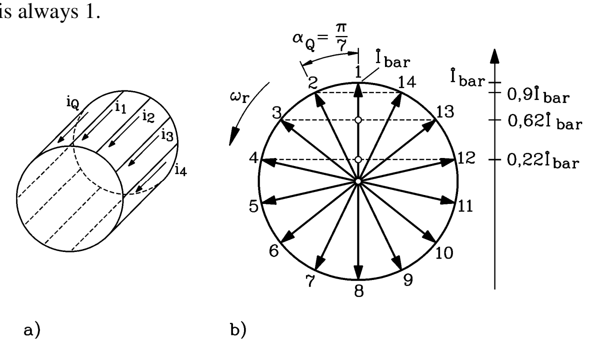

<u>Fig. 3.5:</u> a) Schematic sketch of a squirrel-cage winding, b) symmetrical system of bar currents of a squirrel-cage winding with $Q_r/p = 14$

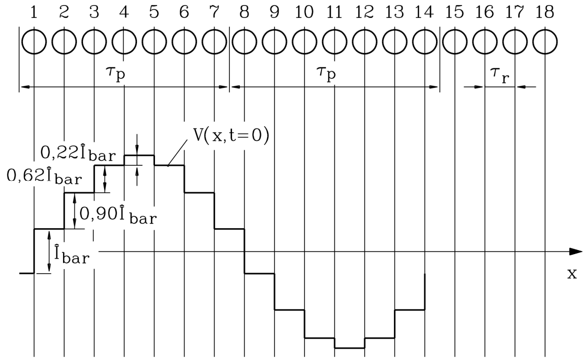

<u>Fig. 3.6:</u> Distribution of the magnetic voltage at the circumference of a machine for a squirrel-cage winding with $Q_r/p = 14$ for the time $t = 0$

<u>*Exercise:*</u> Let the field of Fig. 3.6 "travel" !
You can generate the **travelling of the field** by drawing the distribution $V(x,t)$ for a different time t^*. At this time, the current in bar 1 is about the factor $\cos(\omega_r t^*)$ smaller, the current in bar 2 about the factor $\cos(\omega_r t^* + \alpha_Q)$, the current in bar 3 about the factor $\cos(\omega_r t^* + 2\alpha_Q)$ etc. (Exercise: Choose $\omega_r t^* = \pi/7$!)

3.4 *FOURIER*-Analysis of DC-Excited Rotating Fields

Fig. 3.7 shows the air gap field H_δ of a two-pole, electrically excited rotor of a salient-pole synchronous machine. No current flows in the three-phase winding of the stator (no-load condition). Therefore, this winding is not shown. The openings of the stator slots are neglected. The air gap field is only excited by the ampere-turns of the rotor $N_{fPol} \cdot I_f$, where N_{fPol} is the number of turns per pole. The exciting coils of the north and south pole are – as general done – electrically connected in series. However, the **air gap $\delta(x)$ width is not constant**, because of the shape of the pole shoe and the inter-pole gap. Hence it increases towards the inter-pole gaps. It is a function of the circumferential coordinate x.

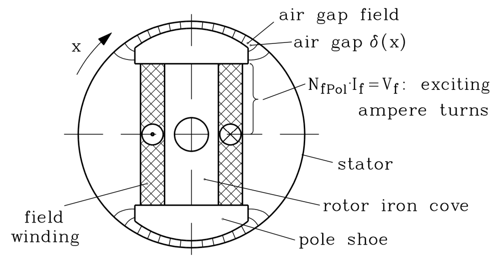

<u>Fig. 3.7:</u> Air gap field of a two-pole synchronous machine at no-load without influence of stator slotting

The iron is assumed to be of infinite permeability ($\mu_{Fe} \to \infty$). Therefore, the magnetic field in the iron parts H_{Fe} is zero. The radial component B_δ of the air gap field is calculated using *AMPERE*'s circuital law.

$$\oint_C \vec{H} \cdot d\vec{s} = 2N_{fPol} I_f = 2V_f = 2H_\delta \delta(x) + 2H_{Fe}\Delta_{Fe} = 2H_\delta \delta(x) \tag{3.48}$$

$$B_\delta(x) = \mu_0 H_\delta(x) = \mu_0 \frac{V_f}{\delta(x)} \tag{3.49}$$

Here, the integration loop C equals a closed loop of a field line of the no-load field $\vec{B}$. As north and south pole do have the same geometry, the function of the field distribution (3.49) is symmetrical to the abscissa $B_\delta(\gamma) = -B_\delta(\gamma + \pi)$ (Fig. 3.8). Therefore, the *FOURIER*-cosine-series consists only of harmonics with odd ordinal numbers.

$$B_\delta(\gamma) = \sum_{\mu=1,3,5,...}^{\infty} \hat{B}_{\delta\mu} \cos(\mu\gamma) \tag{3.50}$$

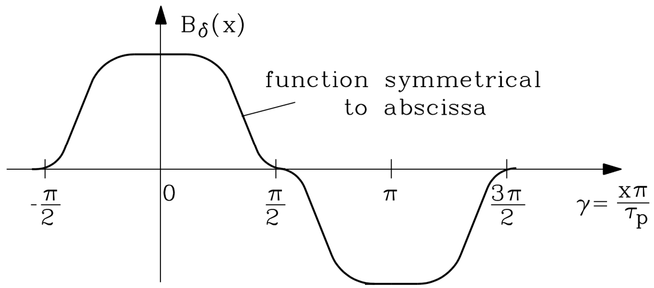

Fig. 3.8: Field distribution $B_\delta(x)$ symmetrical to the abscissa along the circumferential coordinate x at variable air gap $\delta(x)$

The **field distribution** is given by the function of the air gap $\delta(x)$, and hence by the shape of the pole shoe. The field distribution is not sinusoidal as desired, due to the inter-pole gap. This results in **amplitudes of the harmonics** $\hat{B}_{\delta\mu}$ **for $\mu > 1$ different from zero** (In this case, also ordinal numbers exist, that are multiples of 3 !).

The field distribution of Fig. 3.8 – excited by the dc-current I_f – is a dc-field when seen from the rotor. As the rotor rotates with **constant mechanical angular speed** $\Omega_m = 2\pi n = 2v_m/d_{si}$, it is a **rotating field** when seen from the stator winding. Here, v_m is the circumferential speed of the field in the stator bore d_{si}. The circumferential angle γ_r in the coordinate system of the rotor (measured in electric degrees) increases – seen from the circumferential angel γ_s in the coordinate system of the stator – by the angle of rotation $\gamma(t)$. With $\Omega_m = d\gamma_m / dt = (d\gamma / dt)/p$, it is

$$\gamma_s(t) = \gamma_r + \gamma(t) = \gamma_r + \int_0^t d\gamma / dt \cdot dt = \gamma_r + \int_0^t p \cdot \Omega_m \cdot dt = \gamma_r + p \cdot \Omega_m \cdot t \quad . \tag{3.51}$$

Result:
The field waves that are seen as stationary from the rotor are rotating field waves when seen from the stator.

$$B_{\delta\mu}(\gamma_r) = \hat{B}_{\delta\mu} \cdot \cos(\mu\gamma_r) = \hat{B}_{\delta\mu} \cdot \cos(\mu\gamma_s - \mu p \Omega_m t) = \hat{B}_{\delta\mu} \cdot \cos(\frac{\mu\pi x}{\tau_p} - \omega_\mu t) \tag{3.52}$$

At each point x along the circumference of the stator, these field waves generate a change of the magnetic flux density with the frequency

$$f_\mu = \frac{\omega_\mu}{2\pi} = \frac{\mu p \Omega_m}{2\pi} = \mu \cdot p \cdot n \quad . \tag{3.53}$$

This means:
As all rotating waves B_μ pass the stator with the same velocity v_m, the frequency of the μ^{th} harmonic is μ-times as large as the fundamental with $\mu = 1$. These harmonics induce voltages with higher frequencies in addition to the desired sinusoidal voltage of the fundamental. These harmonics may e.g. interfere with neighbouring telephone circuits via electromagnetic interference remarkably. Therefore, the harmonics of the rotor have to be kept as small as possible.

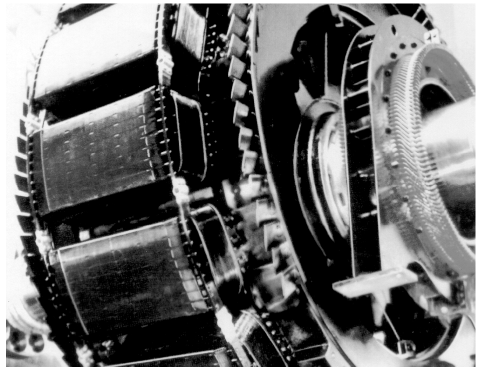

Fig. 3.9: View of the poles of the rotor of a salient-pole synchronous machine